

Depths of cracks produced by abrasion of brittle materials

S.G. Roberts

Dept. Materials, University of Oxford,

OX1 3PH, UK

Introduction

Free-particle abrasion (“lapping”) and grinding with fixed-grit wheels is an important process in stock removal and shaping of ceramic and glass components and semiconductor wafers. Such abrasion is generally thought to remove material from the surface by the production of lateral chips from the sides of plastic grooves formed during by the dragging of abrasive particles across the surface (Figure 1). Several authors have produced models of this process [1,2], and some experimental work has been carried out to verify the predictions of such models [3]. Other authors [4] have focussed on the strength and depth of the residual stress field produced in the surface by the “plastic zones” surrounding the scratch tracks.

Very little work either theoretical or experimental, appears to have been done on the depths of the cracks normal to the surface produced by the abrasive particles. These cracks are analogous to the “median / radial” cracks produced by sharp indentation [5,6]. Such cracks may be important for two reasons: (a) they can act as “Griffith flaws”, reducing the strength of the component [7]; (b) any subsequent stage of finishing with finer grits will need to remove material at least to the depths of these cracks, to avoid unnecessary strength degradation or a poor surface finish.

It appears to be “received wisdom” that the depth of cracking damage produced by free particle abrasion in brittle solids is roughly equal to the diameter of the abrasive particles producing it. Experimental work to confirm this is very sparse. Some experimental work [8-10] has been done on the damage produced by single-point indenters dragged across ceramic surfaces, but in these cases the size of the cracks produced depends on the load applied; there is no inherent dimensional scale equivalent to the abrasive particle size in such experiments. Evans and Wilshaw [1] indented various transparent brittle materials with spheres (and sharp indenters), but focused on the load variation of crack lengths, rather than limiting cases related to the size of the contacting sphere (though the maximum crack

depth produced in ZnS was ~40% of the indenter diameter, at ~30% indenter penetration). Work on “damage-free machining” of brittle materials has largely concentrated on the load or scale of single point contact beneath which lateral or median cracking is not found and thus where machining can be carried out by plastic “turning” processes equivalent to those in metals [11,12].

Such work as has been carried out to determine the depths of cracks under abrasion tracks does seem to confirm the “received wisdom”. Direct measurements are few. Stickler and Booker [13] performed cross-section and plan-view TEM on silicon abraded by various treatments and found that the depth of damage was about 30% of the abrasive particle diameter. For the finest abrasive used, 0.25 μm diamond, only dislocations were produced; the next largest abrasive, 6 μm diamond, produced both dislocations and cracks. Xu, Wei and Jahanmir [14] performed cross-section microscopy on Si_3N_4 abraded by a wheel containing 160 μm diameter diamond grits, and found cracks of ~120 μm depth running normal to the surface beneath the scratch grooves.

There is some indirect evidence of flaw depths, from the strengths of ceramics ground or lapped with abrasives, though conclusions from such data are rendered somewhat tentative by possible effects of residual stresses, interactions with grain structure, inaccurately known K_{Ic} values etc. Mould and Southwick [15] reported strength data for soda-lime glass abraded with SiC particles: the corresponding Griffith flaw sizes are close to the diameters of the grits used. Strength data on ground SiC [16] indicate critical flaws sizes very close to the diameter of the diamond grits used, rather than to the grain size of the SiC; similar conclusions were reached as a result of similar experiments on polycrystalline alumina [17]. In polycrystalline MgO, it also was found that grits introduced flaws of a depth between 100% and 20% of the grit diameter [18]. In Malkin and Ritter’s review of ceramic grinding [19], they note that relationships for crack depths and strength degradation in ceramics due to grinding, analogous to those for indentation fracture mechanics, had not been developed.

The purpose of this paper is to outline a fracture mechanics treatment of the process of “median/radial” cracking of brittle materials by abrasive grits. The depths of the cracks produced are necessarily limited by the size of the grits, since a grit particle cannot transmit a load greater than that needed to embed it completely in the surface being abraded and the counterface. The treatment is necessarily general and approximate because of the large number of unknowns in any real situation, most importantly the likely wide variation in grit shapes.

Simple model for crack depth

We model the abrasive particle as being equivalent to a sharp indenter penetrating the surface. For such indenters, the depth of the median cracks produced has been calculated by various authors (see [20,21] for a survey). One of the more commonly used expressions is [22, 23]:

$$c = \left[\alpha P \left(\frac{E}{H} \right)^{\frac{1}{2}} K_{Ic}^{-1} \right]^{\frac{2}{3}} \quad (1)$$

where P is the applied load, and E , H and K_{Ic} are the Young's modulus, hardness and fracture toughness of the material indented. α is a geometric parameter, found experimentally to be equal to 0.0154 for the case of a Vickers profile indenter for a wide range of materials [23]. Assume that the depth of a crack produced by an abrasive grit, pushed into a surface of a given E , H and K_{Ic} with load P is close to that given by the above expression with $\alpha = 0.0154$. This is justified, to a first approximation, as the driving force for crack extension is the point load P , and should not depend strongly on indenter shape once the cracks are largely outside the indentation's plastic zone, which for hard materials is only slightly bigger than the indentation itself.

We now need to determine P . The normal relations between hardness and indentation size, measured as the indentation area, A , or the radius of the indentation, r , is:

$$H = \frac{P}{A} = \frac{P}{\beta r^2}, \quad (2)$$

where β is a geometrical factor, equal to π for a circular indentation (or 2.16 for a Vickers indentation). For a free abrasive grit of radius R , pushed onto a surface with hardness H by a counterface of identical material (this constraint will be relaxed later), the maximum possible value of P is determined by the force need to embed the grit between the counterface and the abraded surface (see figure 2a), so that $r = R$:

$$P_{\max} = \beta H R^2, \quad (3)$$

Combining equations (1) and (3), we arrive at an expression for the depth of the deepest cracks, c_{\max} :

$$c_{\max} = R^{\frac{4}{3}} \left[\alpha \beta (E H)^{\frac{1}{2}} K_{Ic}^{-1} \right]^{\frac{2}{3}} \quad (4a)$$

or:

$$c_{\max} = \omega R^{\frac{4}{3}}, \quad (4b)$$

where ω is a material-dependent (and, to a lesser extent geometry-dependent) constant. Values of ω (to 2s.f.) for typical brittle materials, with counterfaces of the same material, are given in Table I. The maximum crack depths (to 2s.f.) resulting from abrasion with free abrasives between identical surfaces are given in Table II; note that abrasive particle *diameter* rather than radius is used in this table as this is the figure normally quoted in sizing abrasives. The crack depths predicted are of the order expected from the limited number of experiments that have been done – i.e. about the size of the grit used.

Effect of applied load

Equations 2 and 3 assume that the grit is itself undeformed, and that the load on each grit particle is such as to embed it completely between the two surfaces. These conditions may easily be met in practice, as is discussed below.

It is usually assumed that if the hardness of the “indenter” is greater than that of the substrate by ~25-30%, then it will be undeformed plastically (this is essentially the basis of the Moh’s hardness scale). Of the commonly used abrasives, diamond grits ($H = \sim 100 \text{ GPa}$) will meet this criterion even for SiC ($H = \sim 30 \text{ GPa}$), SiC will meet the criterion for most materials except diamond and boron nitride, and alumina grits ($H = \sim 16 \text{ GPa}$) meet the criterion for materials softer than silicon.

The *average* load on each grit particle between flat surfaces may be estimated by assuming that the load applied to the specimens being abraded is completely supported by the grits. If we assume a “coverage factor”, f , which expresses the average spacing between grit particles in terms of their diameter (such that $f=1$ implies that the grit particles are touching, $f=5$ implies that each grit particle is separated from the next by 5 grit diameters, etc.), then the average load applied through each particle, P_{mean} , is given by:

$$P_{\text{mean}} = \frac{P_{\text{app}} \pi (fR)^2}{A} \quad (5)$$

where P_{app} is a load applied to a specimen of area A . Since P_{max} also varies with R^2 (eqn. 2), we can estimate $P_{\text{mean}} / P_{\text{max}}$ (taking $\beta = \pi$)

$$\frac{P_{\text{mean}}}{P_{\text{max}}} = \frac{P_{\text{app}} f^2}{HA} \quad (6)$$

Typically, in a laboratory situation, P_{app} is between 1 and 100 N, and A is between 5 and $10 \times 10^{-4} \text{ m}^2$. For even the most heavily loaded situation $P_{mean}/P_{max} = 1$ only for $f > 150$ for silica, and at higher values of f for harder materials. These would appear to be sparser distributions of abrasive grits than are likely to occur in real situations; it might therefore be concluded that the situation considered above, giving rise to P_{max} and c_{max} , will never arise. However, on roughened surfaces, grits are likely to be trapped between asperities, giving rise to high local loads. Also, variations in grit size are likely to mean that only a few grits may be loaded at any given time. If only low loads are applied, as may be the case in “finish polishing”, then severe events giving rise to cracks of size c_{max} may be rare. However, for the aggressive abrasive conditions used for stock removal, these “worst cases” may well be frequent enough to give rise to a high density of flaws of size c_{max} .

Effect of counterface

Crack depths will vary with counterface hardness for counterfaces either harder and softer than the material being abraded. Consider the situation where an abrasive grit is pressed between two surfaces of different hardness values, H_s for the abraded surface and H_c for the counterface (Figure 2b). The same load, P , will be applied to the indentation process into the two surfaces, so that the depths of penetration into the surface being abraded, h_s , and the counterface, h_c , are approximately:

$$\frac{h_s}{h_c} = \left(\frac{H_c}{H_s} \right)^{\frac{1}{2}} \quad (7)$$

In the limit of the counterface and abraded surface coming together with the abrasive grit being fully contained between them:

$$h_s + h_c = 2R \quad (8)$$

so that:

$$\frac{H_c}{H_s} = \frac{h_s^2}{(2R - h_s)^2} \quad (9a)$$

$$h_s = 2R \left(1 + \left(\frac{H_s}{H_c} \right)^{\frac{1}{2}} \right)^{-1} \quad (9b)$$

To find P_{max} in the abraded surface, we will apply equation (3). However, a relation between h , the depth of penetration, and r , the indentation radius, is needed to proceed further. While an “exact” relation could be used

(assuming the abrasive grits to be spherical), this is geometrically rather more complex than is justified by other assumptions in the model; the relation between penetration depths and the hardness values involved are not likely to be simple at these situations where the depths of penetration are comparable to the abrasive grit size. At high loads, the grit will start to penetrate the softer surface to a depth greater than its radius (figure 2c). Clearly P_{\max} is limited by the maximum possible depth of penetration, $2R$. P_{\max} is then likely to be controlled by the work-hardening behaviour of the softer material; however, a reasonable upper limit is the load need to make a “normal” indent of depth $2R$, i.e. four times that to make an indent of radius R in the softer material (Figure 2c).

To simplify matters, we will assume a linear relation between h and r , this being equivalent to mutual indentation of materials of constant hardness by an abrasive grit in the form of two cones placed base to base: χ . The ratio $r : h$ reflects the apex angle of the cones to which the abrasive grit is being approximated. Thus:

$$P_{\max} = \chi^2 \beta h_s^2 H_s \quad (10a)$$

$$P_{\max} = \chi^2 \beta r^2 \left(1 + \left(\frac{H_s}{H_c} \right)^{\frac{1}{2}} \right)^{-2} H_s \quad (10b)$$

χ can be estimated by considering limiting cases. If $H_s = H_c$, we would expect to reproduce the result of eqn. 3; if $H_s \gg H_c$, we would expect $P_{\max} = 0$; if $H_s \ll H_c$, we would expect $P_{\max} =$ four times that given by eqn. 3, as discussed above. If $\chi = 2$, all these limiting criteria are met. To get the crack depth in the abraded surface, we then substitute P_{\max} into eqn. (1):

$$c = \left[4\alpha\beta R^2 \left(1 + \left(\frac{H_s}{H_c} \right)^{\frac{1}{2}} \right)^{-2} (H_s E)^{\frac{1}{2}} K_{Ic}^{-1} \right]^{\frac{2}{3}} \quad (11)$$

It should be stressed that this expression is only a “first approximation”; nonetheless, its predictions for typical materials show the expected behaviour patterns. Figure 3 shows the predictions of eqn. 11 for soda-lime glass (“SiO₂”), silicon and alumina abraded by grits of various sizes against counterfaces of different hardness values. For very soft counterfaces, the predicted crack size is very small: as the hardness of the counterface increases, the predicted crack depth rises to a limiting value. The predicted crack depths in the mid- range are approximately the same as the grit diameter, varying somewhat with the elastic modulus and fracture toughness of the material being abraded.

Minimum load for fracture

There is a further limitation on the possible crack sizes produced by abrasion of this type, particularly for small abrasive grit sizes or for very soft counterfaces. Lawn and Evans [24] showed that there is a minimum load (P^*) required to produce any median / radial fracture at all from a point contact, producing a crack of depth c^* . Their analysis produced expressions for c^* and P^* :

$$c^* = \frac{1.767}{\theta^2} \left(\frac{K_{Ic}}{H} \right)^2 \quad (12)$$

$$P^* = \frac{54.47\beta}{\pi\eta^2\theta^4} \left(\frac{K_{Ic}}{H} \right)^3 K_{Ic} \quad (13)$$

where β is a constant relating hardness to indentation diagonal (as defined in eqn. 1 here) and η and θ are geometrical constants; $\theta \approx 0.2$ and $\eta \approx 1$ for a Vickers profile indenter [24]. These equations give values of P^* and c^* as shown in Table 1. These will probably be of the right order for the relatively shallow impressions produced by rounded abrasive grits (both P^* and c^* will be lower for sharper contacts, where θ will be higher). This “minimum load for fracture” is increasingly important with the materials of higher fracture toughness, such as alumina. Cook and Pharr [6] note that the Lawn and Evans analysis may underestimate P^* and c^* , especially for glasses, and review a number of experimental studies to determine P^* and c^* in such materials.

Summary and Conclusions

A simple analysis, based on indentation fracture mechanics, has been used to study the likely maximum depths of cracks normal to the surface in a ceramic material subjected to abrasion by hard particles. The analysis shows that the cracks are likely to be of depths comparable to, and in most cases slightly less than, the diameter of the abrasive particles. This is consistent with the rather limited available experimental data. The depths of cracks produced decrease with decreasing counterface hardness. For very soft counterfaces, the load applied to the surface being abraded may fall below the minimum required to cause any indentation fracture. For harder counterfaces, a limiting value is reached when the abrading grits become completely embedded in the surface being abraded.

Acknowledgements

The author gratefully acknowledges the helpful comments of Dr P D Warren, Dr B. Derby and Dr J T Czernuszka on drafts of this paper.

References

1. Evans, A.G. and Wilshaw, T.R., *Acta Metallurgica*, **24**, 1976, 939
2. Chauhan, R., Ahn, Y., Chandrasekar, S. and Farris, T.N., *Wear*, **162-164**, 1993,, 246.
3. Moore, M.A., *Materials in Engineering Applications*, **1**, 1978, 97.
4. Marshall, D.B., Evans, A.G., Khuri Yakub, B.T., Tien, J.W. and Kino, G.S., *Proceedings of the Royal Society, London*, **385**, 1983, 461.
5. Lawn, B.R. and Wilshaw, T.R., *Journal of Materials Science*, **10**, 1975, 1049.
6. Cook, R.F. and Pharr, G.M., *Journal of the American Ceramics Society*, **73**, 1990, 787.
7. Rice, R.W., in *The Science of Ceramic Machining and Surface Finishing II*, eds. B.J. Hockey and R.W. Rice,, National Bureau of Standards Special Publication 562, U.S. Gov. Printing, Washington D.C., 1979,, pp 429.
8. Broese van Groenou, A., Maan, N. and Veldkamp, J.D.B., *Philips Research Reports*, **30**, 1975, 320.
9. Page, T.F., Sawyer, G.R., Adewoye, O.O. and Wert, J.J., *Proceedings of the British Ceramic Society*, **26**, 1978, 193.
10. Mukhopadhyay, A.K. and Mai, Y.W., *Wear*, **162-164**, 1993,, 258.
11. Puttick, K.E., Rudman, M.R., Smith, K.J., Franks, A. and Lindsey, K., *Proceedings of the Royal Society, London, A*, **426**, 1989, 19.
12. Puttick, K.E., Whitmore, L.C., Chao, C.L. and Gee, A.E., *Philosophical Magazine A*, **69**, 1994, 91.
13. Stickler, R. and Booker, G.R., *Philosophical Magazine*, **8**, 1963, 859.
14. Xu, H.H.K., Wei, L. and Jahanmir, S., *Journal of Materials Research*, **10**, 1995, 3204.
15. Mould, R.E. and Southwick, R.D., *Journal of the American Ceramic Society*, **42**, 1959, 583-592.
16. Cranmer, D.C., Tressler, R.E. and Bradt, R.C., *Journal of the American Ceramics Society*, **60**, 1976, 230.
17. Tressler, R.E., Langensiepen, R.A. and Bradt, R.C., *Journal of the American Ceramics Society*, **57**, 1974, 226.
18. Bradt, R.C., Dulberg, J.L. and Tressler, R.E., *Acta Metallurgica*, **24**, 1976, 529.
19. Malkin, S. and Ritter, J.E., *Transactions of the American Society of Mechanical Engineers: Journal of Engineering for Industry*, **111**, 1989,, 167.
20. Ponton, C.B. and Rawlings, R.D., *Materials Science and Technology*, **5**, 1989, 865.

21. Ponton, C.B. and Rawlings, R.D., *Materials Science and Technology*, **5**, 1989, 961.
22. Lawn, B.R., Evans, A.G. and Marshall, D.B., *Journal of the American Ceramic Society*, **63**, 1980, 574.
23. Anstis, G.R., Chantikul, P., Lawn, B.R. and Marshall, D.B., *Journal of the American Ceramic Society*, **64**, 1981, 533.
24. Lawn, B.R. and Evans, A.G., *Journal of Materials Science*, **12**, 1977, 2195.

Tables

Table 1: Materials parameters

Material	E (GPa)	H (GPa)	K _{Ic} (MPa m ^{1/2})	ω^\dagger (m ^{-1/3})	P* (N)	c* (μm)
Al ₂ O ₃	400	16	4.0	98	3	5
Si	110	10	0.9	147	0.003	0.2
SiO ₂	70	5	0.7	26	0.02	0.6

[†] using $\alpha = 0.0154$, $\beta = \pi$.

Table 2: Predicted maximum crack depths.

Abrasive Particle diameter (μm)	c _{max} (μm)		
	Alumina	Si	SiO ₂
1	0.39	0.58	0.10
2	0.98	1.5	0.26
5	3.3	5.0	0.87
10	8.4	13	2.2
20	21	32	5.5
50	72	107	19
100	180	271	47

Figures

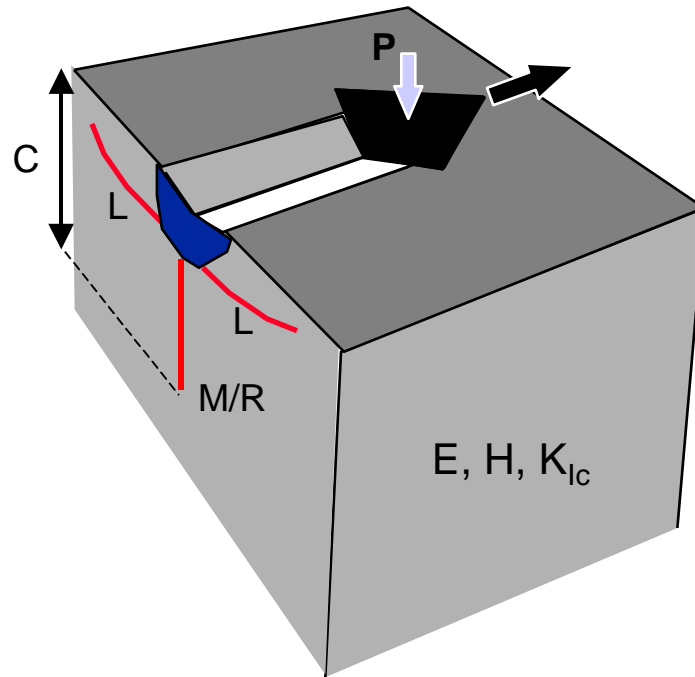


Figure 1: Damage produced by abrasive wear in brittle materials: a plastic groove and subsurface plastic zone, and lateral (L) and median/radial (M/R) cracks.

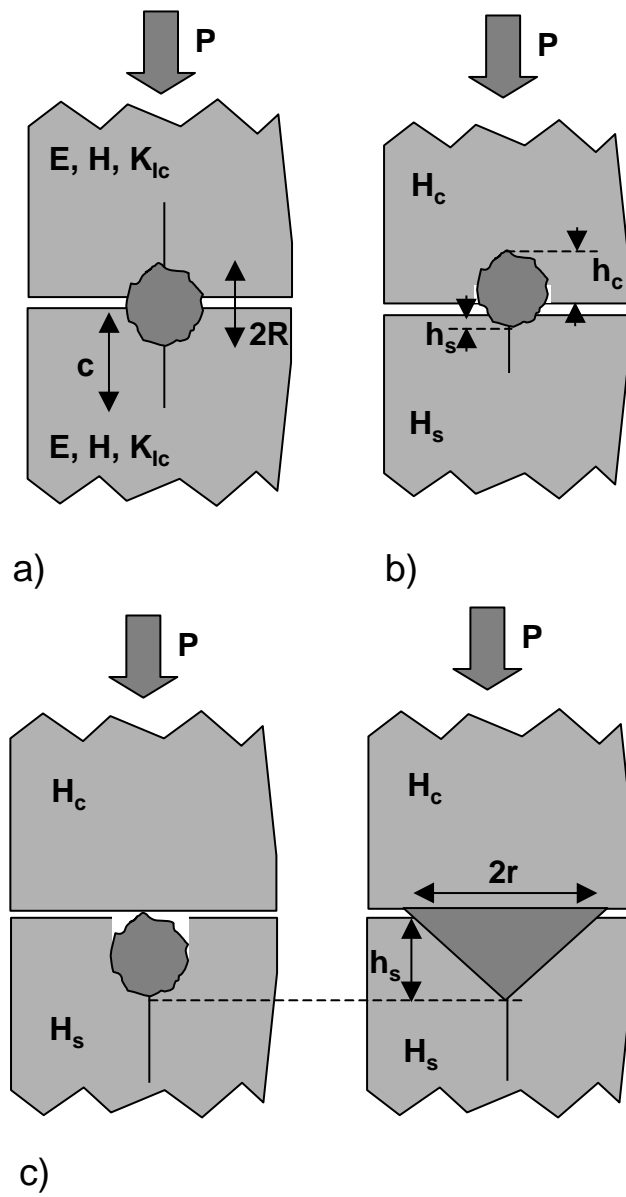


Figure 2: Embedding of abrasive particles between two surfaces.

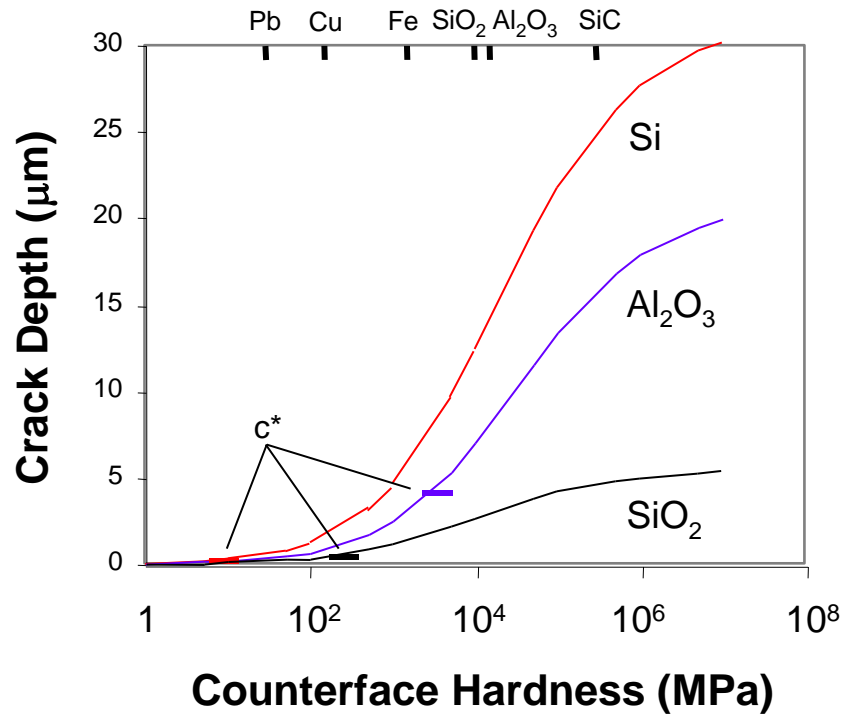


Figure 3: Crack depths in the “abraded surface” of the material indicated from abrasive particles of 10 μm diameter, as a function of counterface hardness. Possible counterfaces are indicated on the upper horizontal axis.